

Article

Investigation into the MOCVD Growth and Optical Properties of InGaN/GaN Quantum Wells by Modulating NH₃ Flux

Zhenyu Chen ^{1,2} , Feng Liang ^{1,*}, Degang Zhao ^{1,3,*}, Jing Yang ¹, Ping Chen ¹ and Desheng Jiang ¹

¹ State Key Laboratory of Integrated Optoelectronics, Institute of Semiconductors, Chinese Academy of Sciences, Beijing 100083, China

² College of Materials Science and Opto-Electronic Technology, University of Chinese Academy of Sciences, Beijing 100049, China

³ Center of Materials Science and Optoelectronics Engineering, University of Chinese Academy of Sciences, Beijing 100049, China

* Correspondence: liangfeng13@semi.ac.cn (F.L.); dgzhao@semi.ac.cn (D.Z.)

Abstract: In this study, the surface morphology and luminescence characteristics of InGaN/GaN multiple quantum wells were studied by applying different flow rates of ammonia during MOCVD growth, and the best growth conditions of InGaN layers for green laser diodes were explored. Different emission peak characteristics were observed in temperature-dependent photoluminescence (TDPL) examination, which showed significant structural changes in InGaN layers and in the appearance of composite structures of InGaN/GaN quantum wells and quantum-dot-like centers. It was shown that these changes are caused by several effects induced by ammonia, including both the promotion of indium incorporation and corrosion from hydrogen caused by the decomposition of ammonia, as well as the decrease in the surface energy of InGaN dot-like centers. We carried out detailed research to determine ammonia's mechanism of action during InGaN layer growth.

Keywords: InGaN quantum well; surface morphology; NH₃ flux; GaN lasers; MOCVD



Citation: Chen, Z.; Liang, F.; Zhao, D.; Yang, J.; Chen, P.; Jiang, D. Investigation into the MOCVD Growth and Optical Properties of InGaN/GaN Quantum Wells by Modulating NH₃ Flux. *Crystals* **2023**, *13*, 127. <https://doi.org/10.3390/cryst13010127>

Academic Editors: Francisco M. Morales and Dmitri Donetski

Received: 28 November 2022

Revised: 26 December 2022

Accepted: 4 January 2023

Published: 10 January 2023



Copyright: © 2023 by the authors. Licensee MDPI, Basel, Switzerland. This article is an open access article distributed under the terms and conditions of the Creative Commons Attribution (CC BY) license (<https://creativecommons.org/licenses/by/4.0/>).

1. Introduction

InGaN/GaN multiple quantum well-based light emitting devices have attracted a large amount of attention during the past few years, especially in the wavelength range of blue and green [1–4]. It is necessary to manufacture high-performance green InGaN/GaN active regions through metal–organic chemical vapor deposition (MOCVD), as they have promising applications in laser display and solid-state lighting [4,5]. However, when an emitting wavelength of an active region is in the green range, the quality of the active region seriously decreases due to a large increase in indium content in the InGaN layer [6].

The incorporation of indium into InGaN is sensitive to several growth conditions, such as temperature, growth rate, flux of sources, pseudo-template characteristic effect, etc. [7,8]. Ammonia is an important gas source in the MOCVD-based growth of GaN-based materials; usually, an increase in the ammonia flow rate is considered to have a positive effect on indium incorporation, because a high V/III ratio is often beneficial to the incorporation of group III atoms [9,10]. However, in this study, we found that ammonia may have a more complicated effect on growth in the InGaN/GaN active region, including on both the optical and structural properties of quantum wells. When the ammonia flow rate was increased to a certain degree, a corrosive effect of ammonia on the InGaN layer was observed. We carried out further studies to explore the interaction mechanism between ammonia and the InGaN layer and its significant influences on the properties of quantum wells. In this work, different ammonia flux during quantum well growth resulted in different emission mechanisms. Analysis on those different emission mechanisms may be beneficial for high quality green InGaN quantum well growth.

2. Experiments

Four InGaN/GaN multi-quantum-well (MQW) samples (series I, A, B, C, and D) and five InGaN/GaN single-quantum-well (SQW) samples (series II, S1, S2, and S3; and series III, R1 and R2) were grown on 2 inch c-plane (0001) sapphire substrates via a Thomas Swan MOCVD with close-coupled showerhead reactor. During MOCVD growth process, trimethylindium (TMIn) and trimethylgallium (TMGa) were employed as the metal precursors for gallium and indium, and ammonia (NH₃) acted as the nitrogen precursor. Hydrogen was used as the carrier gas for the quantum well structure (including quantum wells and quantum barriers) growth and nitrogen was used as carrier gas for all the other layers. Bicyclopentadienyl magnesium (Cp₂Mg) and silane were used for p- and n-type doping, respectively.

The epitaxial structure of the MQW samples in series I consisted of a 23 nm GaN nucleation layer; a 1.5 μm, unintentionally doped GaN layer; a 1 μm, Si-doped n-GaN layer (electron concentration = $3.5 \times 10^{18} / \text{cm}^3$); a 2-period InGaN (3 nm)/GaN (8 nm) MQW active region; a 1 μm, Mg-doped p-GaN layer (hole concentration = $2.1 \times 10^{17} / \text{cm}^3$); and a 40 nm, p++ type GaN layer. The epitaxial structure was then annealed in nitrogen gas at 800 °C for 180 s. The epitaxial structure of the SQW samples in series II did not have P-type layers, and no annealing process was carried out after the epitaxial growth was realized. The structure of these samples consisted of a 23 nm GaN nucleation layer; a 1.5 μm, unintentionally doped GaN; a 1 μm, Si-doped n-GaN layer; and an InGaN (3 nm)/GaN (8 nm) SQW. Samples in series III were grown under the same conditions as those in series II, except a p-type layer was grown above the SQW region, and afterwards, they underwent an annealing process. All the film thicknesses were controlled by post-growth analysis via HRXRD to ensure different samples in the same series have the same thickness for each layer.

The growth conditions for all 4 MQW samples in series I were the same, except for the NH₃ flow rate during quantum well growth, which was different, being 1, 2, 3, and 4 slm for samples A, B, C, and D, respectively. V/III-ratios of these samples were 6800, 13,600, 20,400 and 27,200 corresponding to the different ammonia flow rates. The SQW samples in series II were grown under the same conditions as those in series I, and the NH₃ flow rate was 1, 2, and 4 slm for samples S1, S2, and S3, respectively. The samples in series III were grown under different NH₃ flow rates: 2 and 4 slm for samples R1 and R2. The schematic diagrams for the InGaN/GaN MQW and SQW samples are shown in Figure 1, and the growth conditions are shown in Table 1. In this work, modulating ammonia flux did not result in an obvious growth rate change. Samples in the series I share similar film thickness for each layer as results of HRXRD shown.

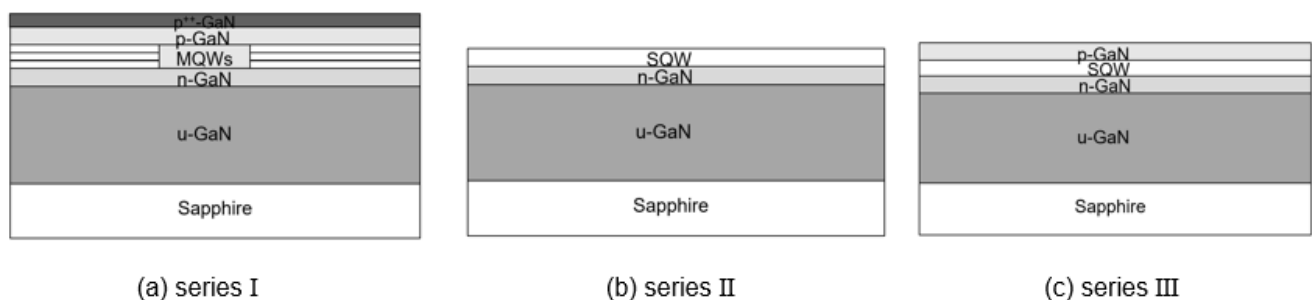


Figure 1. Schematic diagrams for InGaN/GaN MQW (series I) and SQW (series II/III) samples.

The samples in series I were characterized via high resolution X-ray diffraction (HRXRD), electroluminescence (EL) spectroscopy and temperature-dependent photoluminescence (TDPL) spectroscopy measurements. An in-plane scan was performed via HRXRD, employing a Cu K α 1 line. The EL spectra were recorded using a high-resolution spectrometer using a direct current injection. The TDPL spectra were recorded from 30K to 300K using a 405 nm GaN semiconductor laser as the excitation source. Micro-PL images

were taken under a confocal microscope with a 405 nm GaN semiconductor laser as the excitation source. Samples in series II and III were analyzed using an atomic force microscope (AFM) in a surface morphology test.

Table 1. Quantum well growth conditions for different samples of series I, II, and III with varying ammonia flow rates.

| Series | Sample Name | Temperature (°C) | NH ₃ Flux (slm) |
|--------|-------------|------------------|----------------------------|
| I | A | 665 | 1 |
| | B | 665 | 2 |
| | C | 665 | 3 |
| | D | 665 | 4 |
| II | S1 | 665 | 1 |
| | S2 | 665 | 2 |
| | S3 | 665 | 4 |
| III | R1 | 665 | 2 |
| | R2 | 665 | 4 |

3. Results and Discussions

The HRXRD results for the samples in series I showed that in the four samples, the quantum wells and quantum barriers had the same thicknesses (3 nm and 8 nm, respectively). The electroluminescence (EL) spectra of the samples in series I were measured, and the results are presented in Figure 2. As the current injection increased, the peak wavelengths of all of the samples showed a decreasing trend, as shown in Figure 2a. First, the wavelength of the EL peak increased when the NH₃ flow rate was below 2 slm during the InGaN layer growth, but the peak wavelength decreased with a further increase when the flow rate was over 2 slm, which indicated that the indium content in InGaN quantum wells decreases when the NH₃ flow rate is increased over a certain threshold, as shown in Figure 2b. Previous research has shown that NH₃ may have both positive and negative effects on the incorporation of indium atoms into InGaN quantum wells in the wavelength range of blue LED [11,12]. It has been reported that when InGaN is generated in MOCVD by NH₃, TMIn, and TMGa, an additional reaction of $\text{NH}_3 - \text{NH}_3 \rightarrow (1-x)\text{NH}_3 + x\left(\frac{1}{2}\text{N}_2 + \frac{3}{2}\text{H}_2\right)$ —occurs [13]. The NH₃ dissociation reaction provides more H₂, and it is proved to have a corrosive effect on indium atoms [14,15]. For green InGaN/GaN MQW LDs, the incorporation of indium can be more sensitive to growth conditions due to the higher indium content in InGaN. For the samples in series I, the EL result corresponded well with results that have been previously reported [11,12].

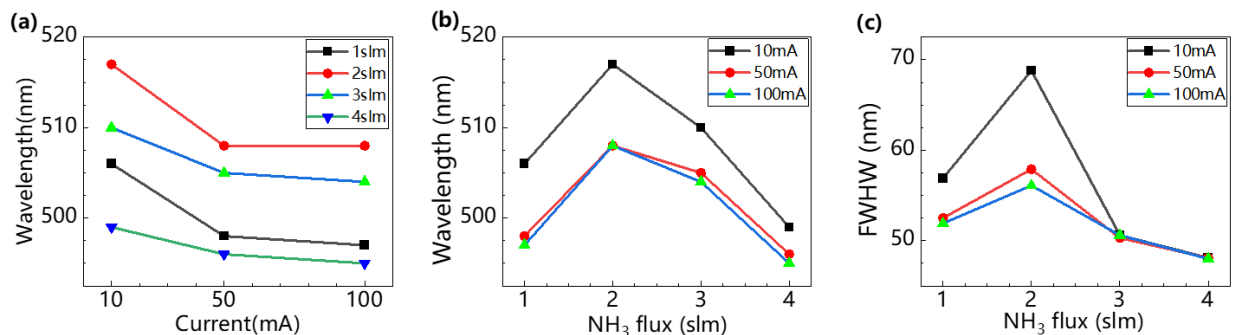


Figure 2. EL peak wavelength vs. injection current and NH₃ flux (a,b); FWHM (c) dependence on varying NH₃ flux measured under different injections of 10, 50 and 100 mA. The lines are connected for visual purposes.

However, a strange increase in the FWHM of the EL spectral peak (10~20 nm higher than other samples) was observed in sample B (grown at 2 slm NH₃ flux), as shown in

Figure 2c. Additionally, a remarkable decrease in the peak wavelength of the EL spectra occurred when the injection current increased from 10 to 50 mA, as shown in Figure 2b. The decreases in samples A and B (approximately 8–9 nm) were a little larger than those in samples C and D. These phenomena indicate that ammonia flux could influence the incorporation of indium into InGaN layers. However, more effects may be caused by the change in NH₃ flux during growth. A set of PL/TDPL measurements of samples A, B, and D were made to characterize the emitting mechanism of InGaN/GaN MQW samples with different NH₃ flow rates, and this is discussed in detail below.

The TDPL spectra data are shown in Figure 3. We attributed the small, undulating peaks observed in Figure 3a–c to interference fringes due to the Fabry–Perot effect of the epitaxial films, and Gaussian fitting was applied to obtain the spectral line shape of the luminescence peak and eliminate the disturbance of interference. The wavelengths of emission peaks shown in Figure 3d–f were collected from Gaussian fitting peaks in Figure 3a–c, respectively. Compared to the EL results in Figure 2, we observed that the TDPL spectra showed totally different luminescence modes in these samples. Because EL testing has a much higher carrier injection than TDPL, the emission peaks in EL spectra were mainly derived from quantum wells, as the intensity of the emission peaks from localized states was much weaker compared to that from quantum wells under high injection conditions. In comparison, TDPL spectra show more information regarding those peaks which may be neglected under high injection conditions. Different luminescence modes were found in samples A, B, and D. In sample B, two main emission peaks were observed, but in samples A and D, only one emission peak was observed. A reasonable explanation for this is that there might have been two different luminescence mechanisms in these three samples, i.e., emissions from QD-like (quantum-dot-like) centers and from quantum wells. A typical emission peak from InGaN QD-like centers has characteristics which include a low spectral width of emission peaks, high intensity at a low injection rate, and low sensitivity to temperature change [16]. For emissions from quantum wells, a larger width of emission peaks and a more sensitive temperature dependence is expected. In sample B, two different emission peaks, PM and PD, were observed. The green emission peak (at 515 nm at 30K, i.e., PM in Figure 3b) had a broader width over 60 nm, and the intensity of this peak decreased sharply with the increasing temperature, especially at the room temperature range, in which this peak was too weak to be detected. Because of the weak emission when the temperature was over 150K, the FWHM and wavelength of this peak may lack accuracy, and the analysis on this peak were all based on the data collected before 150K. Another yellow peak (at 590 nm at 30K, i.e., PD in Figure 3b) had greater intensity, a smaller width around 40 nm, and was more stable when the temperature increased. Thus, these two peaks could be attributed to two different emission origins: the green peak to quantum well emission and the yellow peak to QD-like center emission. When sample A was examined, a high-intensity peak with a small width under 40 nm was detected. Additionally, there was only a slight decrease in the peak intensity with the increase in temperature. The change tendency of the peak wavelength and FWHM (Figure 4a,b) was similar to that of the PD peak in sample B, as the peak wavelength shifting was under 3 nm and the FWHM was lower than 50 nm, indicating that these two peaks should have had similar luminescence mechanisms. Correspondingly, an emission peak with a larger FWHM around 65 nm was found in sample D, and the intensity of this peak decreased rapidly when temperature increased, especially when it increased to the room temperature range (not shown in Figure 3f). The origin of this peak should have been similar to PM. The peak wavelengths of PM and the peak in sample D both had a 5 nm increase when the temperature rose from 30 K to 100 K, and both had a decrease trend when the temperature was over 100 K. However, the temperature dependence of the peak wavelength of PM was quite different from the peak in sample D when the temperature was over 150 K, as can be seen in Figure 3e,f. We think the reason for this could be that the PL peak intensity of PM and sample D decreased rapidly with the increase in temperature, especially when the temperature was over 150 K. As a result, the peak wavelength of

these two peaks could be severely affected by the adjacent peaks, which became clearly stronger. Thus, we determined that in sample A, only QD-like center emissions existed, and in sample D, only quantum well emissions existed. Additionally, the characteristics of the TDPL emission peaks from sample D and PM in sample B under room temperature conditions were consistent with the EL results shown in Figure 2. It can be concluded that in these two cases, the emission mechanism was the same as that in EL testing, in which emissions were derived from the InGaN quantum well matrix. However, there were no such emission peaks in sample A under TDPL, which was consistent with EL spectra. A reasonable explanation for this is that more deep localized states existed in sample A, and then, carrier recombination in QD-like structures predominated under a small injection rate. In comparison, carrier recombination mainly took place in the quantum well matrix under a high injection rate in EL. As a result, the intensity of emissions from QD-like structures was much higher than that from the quantum well matrix under small injection rates, which made it difficult to observe the emissions from the quantum well matrix in TDPL. Additionally, in terms of EL testing, only emissions from the quantum well matrix could be observed, which was the same as that in sample B and D.

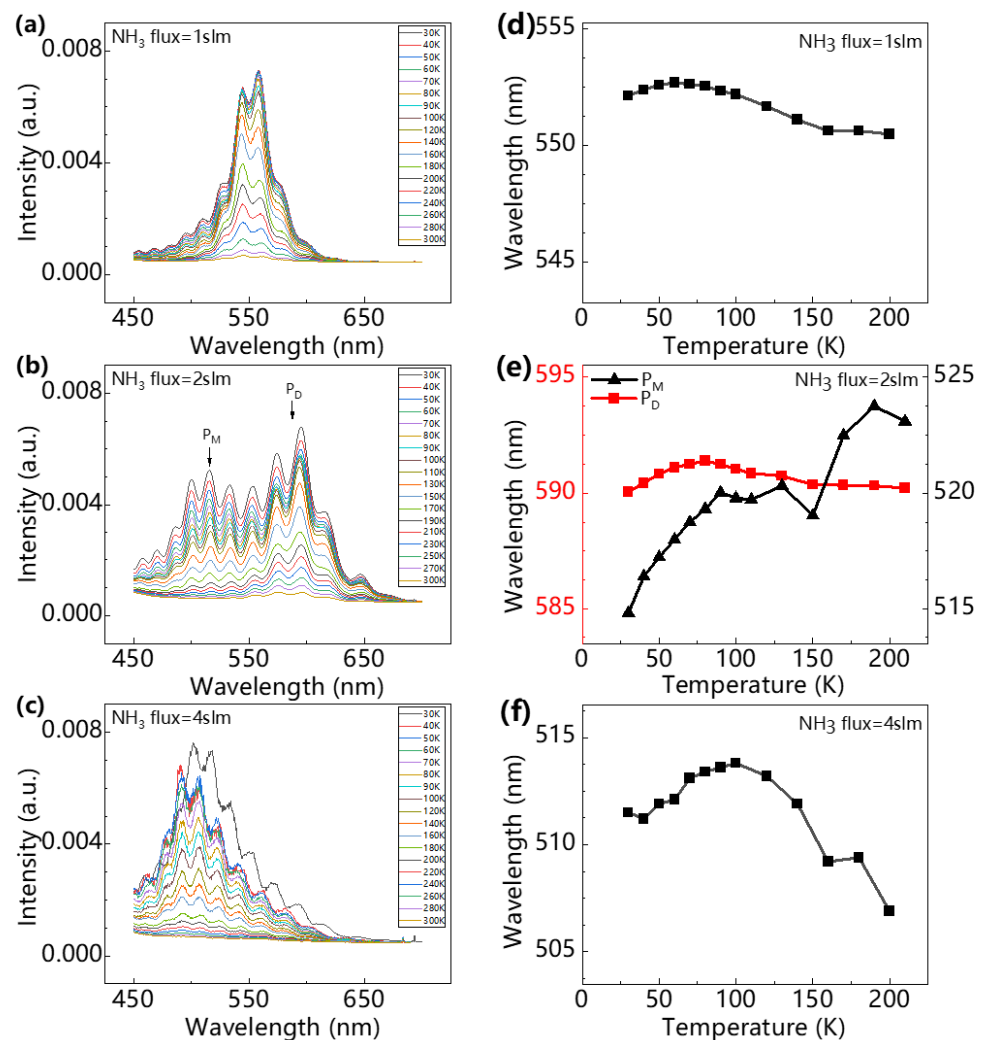


Figure 3. TDPL spectra (a–c) and temperature-dependent emission peak wavelength in series II (d–f) for samples A, B, and D, grown with NH₃ flux of 1, 2, and 4 slm, respectively. In Figure 3 (b,e), PD is assigned to the peak from quantum-dot-like centers, and PM is assigned to the peak from quantum wells. The connected lines in (d–f) are shown for visual purposes.

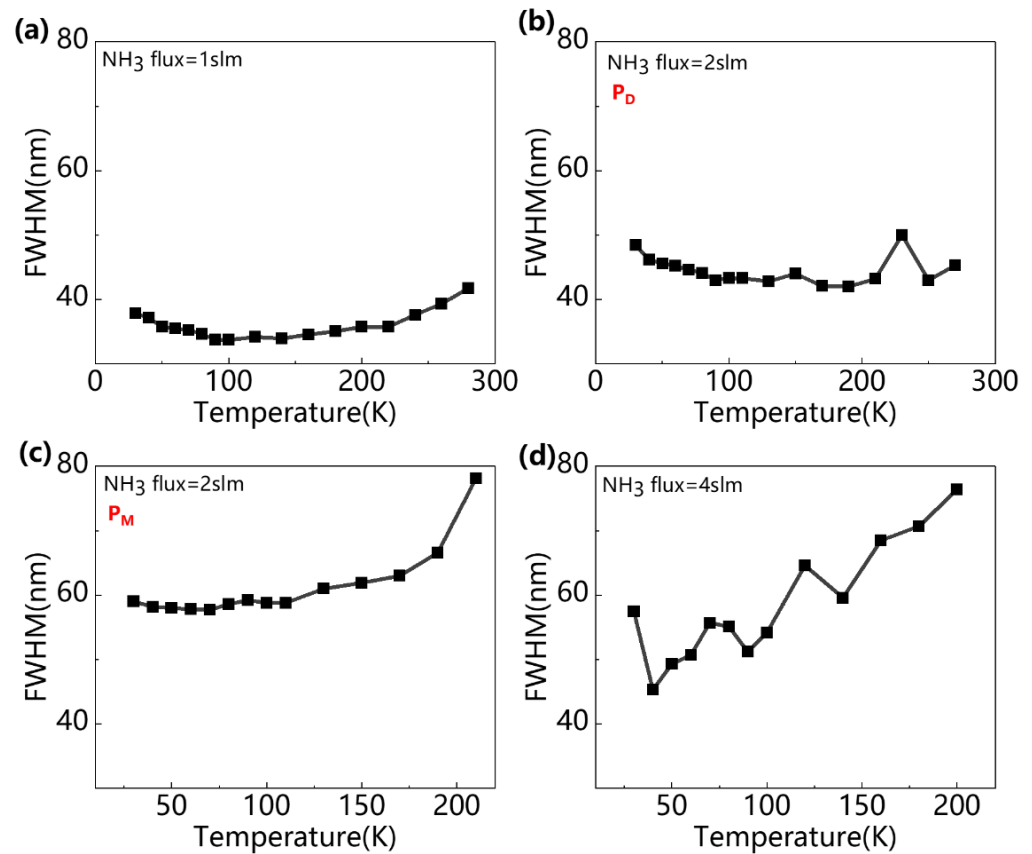


Figure 4. Temperature-dependent full width at half magnitude (FWHM) of PL peaks for samples A, B, and D in series II (a–d) grown with NH_3 flux of 1, 2, and 4 slm, respectively, where PD is marked for the peak from QD-like centers and PM is marked for the peak from quantum wells (b,c). The connected lines are only used for visual purposes.

In order to further examine whether there was a structure in these QWs which may have supplied a composite luminescence mechanism for both QW and QD-like emissions, the samples in series II and series III were tested.

In series II, samples S1, S2, and S3 were prepared based on the growth conditions of samples A, C, and D, respectively. Instead of two-period-MQWs, only a single quantum well was grown in these samples. AFM images of samples in series II are shown in Figure 5, and the height distribution at a cross section of the surface near white spots in Figure 5 is correspondingly shown in Figure 6.

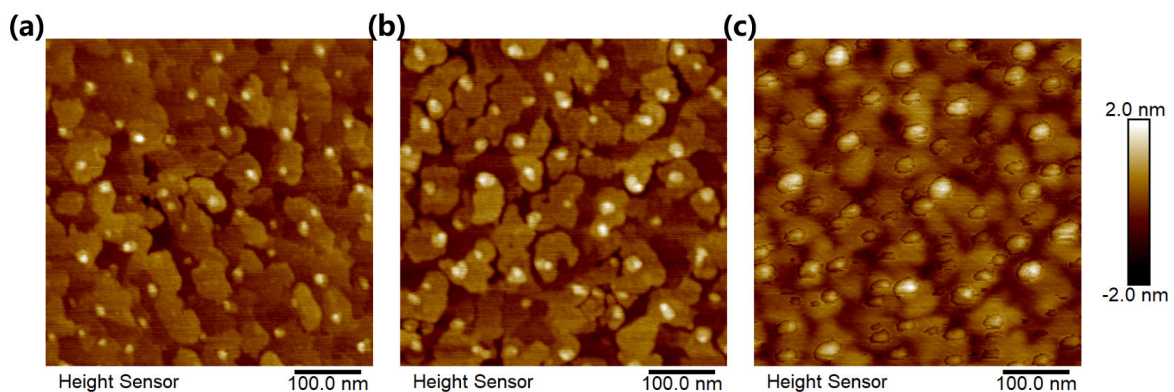


Figure 5. AFM images for samples S1 (a), S2 (b), and S3 (c), where white spots are assigned as QD-like centers.

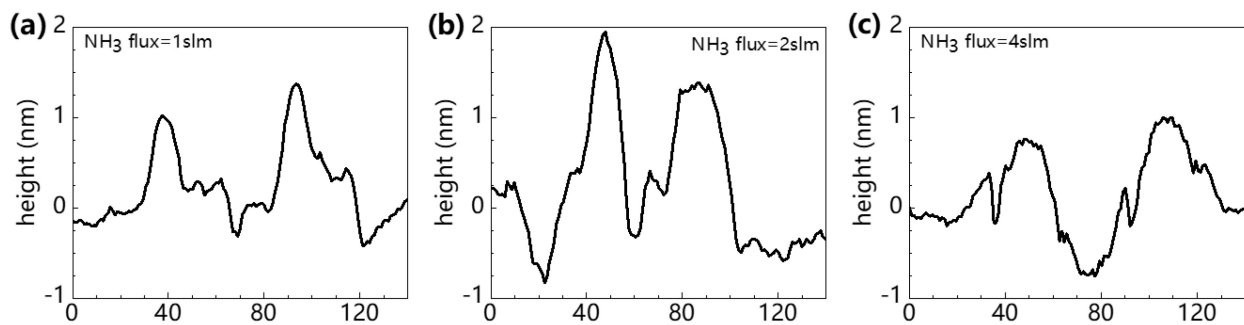


Figure 6. Height distribution at a cross section of the surface near white spots in AFM results for samples S1 (a), S2 (b), and S3 (c), correspondingly.

In all of these three samples, the surface topography suggested Stranski–Krastanov mode growth had a remarkable influence, which allows a 3D nanostructure to grow on a 2D wetting layer [17]. For sample S1 and sample S2, the InGaN epilayers were mainly composed of three parts, i.e., a 2D wetting layer, a 3D large island layer, and large amounts of QD-like centers located above the large islands. However, in sample S3, only mild fluctuations or thick dots could be found on the surface, which looked like flat island aggregates. AFM data show that in comparison to sample S1, sample S2 had QD-like centers with higher densities and larger sizes. The QD-like structures in sample S3 were much shorter and thicker than those in sample S1 and S2 as Table 2 shown.

Table 2. Characteristics of QD-like centers in samples S1, S2, and S3.

| Sample | Density/cm ⁻² | Diameter/nm | Height/nm |
|--------|--------------------------|-------------|-----------|
| S1 | 1.9×10^{10} | 15~20 | 1~2 |
| S2 | 2.7×10^{10} | 20~30 | 1~2 |
| S3 | 2.7×10^{10} | 35~40 | ~1 |

According to a previous report [18], green InGaN/GaN MQW samples often show morphologies with large amounts of islands on the GaN layer with QDs above these islands. The formation of InGaN QDs during epitaxial growth is based on the typical Stranski–Krastanov growth mode [18]. Due to lattice mismatch between InGaN and GaN, the InGaN layer grown on GaN will suffer from a high level of compressive stress, and the strain energy will accumulate during the growth of the InGaN layer. When the thickness of the InGaN layer becomes more than a critical thickness, the transition from 2D to 3D growth mode will occur. Additionally, when the thickness of the InGaN layer becomes even higher, it will meet another critical thickness level at which layer relaxation occurs. Thus, strained QD-like centers will form on the top of the InGaN layer. In addition, the critical thickness of the wetting layer for the formation of QD-like centers decreases when the indium composition of the InGaN layer increases [19,20]. Kobayashi reported an S-K growth mode InGaN layer of 50% indium without the formation of QDs on SiC substrate [21], but it was also reported that strained QDs were observed after a 0.9 monolayer (ML) was grown when growing InN on a GaN substrate [22,23]. We think it may be possible for the growth mode to change from the S-K growth mode to a complete V-W growth mode when the indium composition in InGaN increases from 50% to 100%. It should also be mentioned that when using MBE to epitaxially grow the InGaN layer, the critical thickness of the wetting layer for QD's formation is smaller than that of MOCVD [24,25]. In fact, different surface structures and dynamic processes of MBE and MOCVD will lead to different surface energies, which may result in differences in the critical thicknesses.

Referring to the observed results for samples in series II, ammonia flux during growth had a significant effect on the size and density of QD-like centers. The structural characteristics of QD-like centers in series II samples are listed in Table 2. The density data were calculated by counting white spots in a unit area, and the height and diameter data were

obtained by averaging five height and diameter figures measured from cross section images for each sample. The mechanism of how ammonia flux affects the formation of QD-like centers can be explained from two perspectives.

Firstly, in terms of surface thermodynamics, it was found that when growing InAs self-assembled QDs on the InP substrate, the size of InAs QDs will decrease as the AsH_3 flow rate decreases [26]. A lower flow rate will result in a change in the pressure condition, which makes the surface energy of InAs increase. Higher surface energy supports the formation of smaller-size QDs. Additionally, such a chemical process is also effective in the formation of InGaN QD-like centers in MOCVD.

Secondly, in terms of surface dynamics, when growing GaN using MBE, a higher flow rate of nitride will increase the surface diffusion barrier of gallium atoms [27]. Oliver et al. [28] reported that the diffusion of adatoms on the surface was affected not only by active nitrogen atoms, but also by hydrogen radicals. Hydrogen radicals can be found in the decomposition of ammonia during MOCVD epitaxy. Increasing the flow rate of ammonia or promoting the decomposition of ammonia can decrease the surface diffusion barrier of adatoms, therefore increasing the mobility of adatoms. In conclusion, increasing the ammonia flow rate can increase the size of InGaN QD-like centers by decreasing their surface energy and enhancing the diffusion mobility of indium adatoms.

As a result of these two factors, it was shown that sample S1 had a morphology with smaller QD-like structures, which was more efficient in confining carriers in deep localized states, generating strong emissions with long wavelengths, as presented in TDPL spectra. When the QD-like centers grew thicker with higher ammonia flux, especially over 2 slm, in sample S2 and S3, carriers could not be confined well in such QD-like centers. Thus, more carrier combination took place in the quantum well matrix, leading to weaker emissions at long wavelengths and stronger emissions at short wavelengths, as shown in the TDPL results. Additionally, the characteristics of those stronger emissions at short wavelengths corresponded well with the emission peaks detected in EL testing, which mainly originated in radiative recombination in the quantum well matrix.

In the series III samples, where QD-like centers were formed under a GaN cap layer and underwent an annealing procedure, QD-like centers tended to combine with each other, which made the size of QD-like centers larger, together with a decrease in their density, which can be seen in Figure 7. In sample R1 (Figure 7b), the islands became enhanced as QD-like centers merged with each other. In sample R2 (Figure 7d), the homogeneity of QD-like centers and the layer under them seemed to clearly decrease. Additionally, we speculated that too-large QD-like centers may restrain the QD-like center emissions after the annealing process.

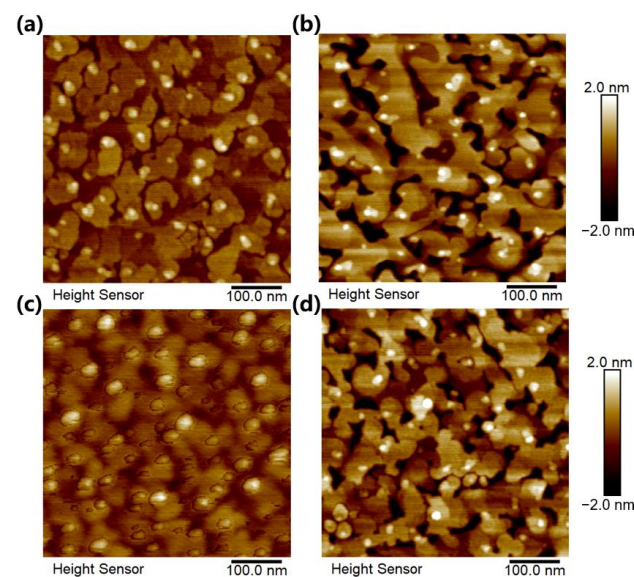


Figure 7. AFM images of sample S1 (a), R1 (b), S2 (c), and R2 (d), where white spots are QD-like centers.

4. Conclusions

In this study, the effects of ammonia flux on the MOCVD epitaxial growth of the InGaN layer and the properties of related InGaN/GaN MQW (or SQW) structures were investigated. The results can be summarized to two aspects. Firstly, ammonia has great influence on the incorporation of indium atoms into InGaN, especially the structural and emission properties of quantum wells. A higher ammonia flow rate leads to a larger V/III ratio, resulting in high nitrogen atom concentration, which is beneficial to the growth of InGaN. With higher nitrogen atom concentration, indium atoms are more likely to incorporate into the InGaN epilayer, resulting in higher indium content in InGaN quantum wells. However, when the ammonia flow rate increases beyond a threshold in which the disassociation of ammonia plays a dominant role, the corrosion of indium caused by extra H₂ generated from ammonia decomposition will decrease the indium content in InGaN, resulting in a blue shift of the emission peak.

It is noted that ammonia has an obvious effect on the surface morphology of the InGaN epilayer. With an ammonia flow rate over 2 slm, surface atoms have higher migration mobility, and the formation of QD-like centers has lower surface energy. These factors lead to thicker and shorter QD-like centers, which are less effective in carrier localization. Based on different conditions of the InGaN layer surface, InGaN MQWs will show two different luminescence mechanisms. In TDPL testing, samples with low ammonia flux presented typical emission peaks of QD-like centers, and samples with high ammonia flux showed typical emission peaks of quantum wells. However, all of the samples showed the emission peaks of quantum wells in EL testing.

Emissions from QD-like centers are remarkable under small injection rates, such as that in PL testing, but when it comes to large injection rates, as in laser diodes, the emissions from the quantum well matrix dominate. Further research is needed to determine whether it is feasible to utilize the emissions from QD-like centers for green laser diodes. However, if we want to optimize the emissions from the quantum well matrix, it is possible to eliminate the effect of QD-like centers by increasing ammonia flux during MOCVD growth. The results of this study regarding the effect of ammonia flux during InGaN MOCVD growth show that it is more promising to grow epitaxially high-performance green laser diodes with InGaN/GaN MQWs.

Author Contributions: Formal analysis, Z.C., F.L. and D.Z.; investigation, Z.C. and F.L.; resources, F.L. and D.Z.; writing—original draft preparation, Z.C. and F.L.; writing—review and editing, D.J., J.Y. and P.C.; supervision, D.Z.; project administration, D.Z.; funding acquisition, F.L., D.Z. and J.Y. All authors have read and agreed to the published version of the manuscript.

Funding: This work was supported by National Key R&D Program of China (Grant No. 2022YFB3608100), Beijing Municipal Science & Technology Commission, Administrative Commission of Zhongguancun Science Park (Z211100007921022, Z211100004821001), National Natural Science Foundation of China (Grant Nos. 62034008, 62074142, 62074140, 61974162, 61904172, 61874175, 62127807, U21B2061), Key Research and Development Program of Jiangsu Province (BE2021008-1), Beijing Nova Program (Grant No. 202093), Strategic Priority Research Program of Chinese Academy of Sciences (Grant No. XDB43030101), and Youth Innovation Promotion Association of Chinese Academy of Sciences (Grant No. 2019115).

Institutional Review Board Statement: Not applicable.

Informed Consent Statement: Not applicable.

Data Availability Statement: The data that support the findings of this study are available from the corresponding author upon reasonable request.

Conflicts of Interest: The authors declare no conflict of interest.

References

1. Baten, M.Z.; Alam, S.; Sikder, B.; Aziz, A. III-Nitride Light-Emitting Devices. *Photonics* **2021**, *8*, 430. [[CrossRef](#)]
2. Sizov, D.; Bhat, R.; Zah, C.E. Gallium Indium Nitride-Based Green Lasers. *J. Light. Technol.* **2012**, *30*, 679–699. [[CrossRef](#)]

3. Liang, F.; Zhao, D.; Liu, Z.; Chen, P.; Yang, J.; Duan, L.; Shi, Y.; Wang, H. GaN-based blue laser diode with 6.0 W of output power under continuous-wave operation at room temperature. *J. Semicond.* **2021**, *42*, 112801. [[CrossRef](#)]
4. Yang, J.; Zhao, D.; Liu, Z.; Liang, F.; Chen, P.; Duan, L.; Wang, H.; Shi, Y. A 357.9 nm GaN/AlGaIn multiple quantum well ultraviolet laser diode. *J. Semicond.* **2022**, *43*, 010501. [[CrossRef](#)]
5. Zhi, T.; Tao, T.; Liu, X.; Xue, J.; Wang, J.; Tao, Z.; Li, Y.; Xie, Z.; Liu, B. Low-threshold lasing in a plasmonic laser using nanoplate InGaIn/GaN. *J. Semicond.* **2021**, *42*, 122803. [[CrossRef](#)]
6. Liang, Y.; Liu, J.; Ikeda, M.; Tian, A.; Zhou, R.; Zhang, S.; Liu, T.; Li, D.; Zhang, L.; Yang, H. Effect of inhomogeneous broadening on threshold current of GaN-based green laser diodes. *J. Semicond.* **2019**, *40*, 052802. [[CrossRef](#)]
7. Wang, X.W.; Liang, F.; Zhao, D.G.; Liu, Z.S.; Zhu, J.J.; Peng, L.Y.; Yang, J. Improving the homogeneity and quality of InGaIn/GaN quantum well exhibiting high indium content under low TMIn flow and high pressure growth. *Appl. Surf. Sci.* **2021**, *548*, 10. [[CrossRef](#)]
8. Benzarti, Z.; Sekrafi, T.; Bougrioua, Z.; Khalfallah, A.; El Jani, B. Effect of SiN Treatment on Optical Properties of In(x) Ga1-x N/GaN MQW Blue LEDs. *J. Electron. Mater.* **2017**, *46*, 4312–4320. [[CrossRef](#)]
9. Kim, S. The influence of ammonia pre-heating to InGaIn films grown by TPIS-MOCVD. *J. Cryst. Growth* **2003**, *247*, 55–61. [[CrossRef](#)]
10. Kunzmann, D.J.; Kohlstedt, R.; Uhlig, T.; Schwarz, U.T. Critical discussion of the determination of internal losses in state-of-the-art (Al,In)GaIn laser diodes. In Proceedings of the Conference on Gallium Nitride Materials and Devices XV, San Francisco, CA, USA, 4–6 February 2020.
11. Yang, J.; Zhao, D.G.; Jiang, D.S.; Chen, P.; Zhu, J.J.; Liu, Z.S.; Liu, W.; Liang, F.; Li, X.; Liu, S.T.; et al. Increasing the indium incorporation efficiency during InGaIn layer growth by suppressing the dissociation of NH₃. *Superlattices Microstruct.* **2017**, *102*, 35–39. [[CrossRef](#)]
12. Yang, J.; Zhao, D.G.; Jiang, D.S.; Chen, P.; Zhu, J.J.; Liu, Z.S.; Liu, W.; Li, X.; Liang, F.; Liu, S.T.; et al. Investigation on the corrosive effect of NH₃ during InGaIn/GaN multi-quantum well growth in light emitting diodes. *Sci. Rep.* **2017**, *7*, 44850. [[CrossRef](#)] [[PubMed](#)]
13. Hirasaki, T.; Hasegawa, T.; Meguro, M.; Thieu, Q.T.; Murakami, H.; Kumagai, Y.; Monemar, B.; Koukitu, A. Investigation of NH₃ input partial pressure for N-polarity InGaIn growth on GaIn substrates by tri-halide vapor phase epitaxy. *Jpn. J. Appl. Phys.* **2016**, *55*, 05FA01. [[CrossRef](#)]
14. Czernecki, R.; Kret, S.; Kempisty, P.; Grzanka, E.; Plesiewicz, J.; Targowski, G.; Grzanka, S.; Bilska, M.; Smalc-Koziorowska, J.; Krukowski, S.; et al. Influence of hydrogen and TMIn on indium incorporation in MOVPE growth of InGaIn layers. *J. Cryst. Growth* **2014**, *402*, 330–336. [[CrossRef](#)]
15. Czernecki, R.; Grzanka, E.; Smalc-Koziorowska, J.; Grzanka, S.; Schiavon, D.; Targowski, G.; Plesiewicz, J.; Prystawko, P.; Suski, T.; Perlin, P.; et al. Effect of hydrogen during growth of quantum barriers on the properties of InGaIn quantum wells. *J. Cryst. Growth* **2015**, *414*, 38–41. [[CrossRef](#)]
16. Wang, L.; Wang, L.; Yu, J.; Hao, Z.; Luo, Y.; Sun, C.; Han, Y.; Xiong, B.; Wang, J.; Li, H. Abnormal Stranski-Krastanov Mode Growth of Green InGaIn Quantum Dots: Morphology, Optical Properties, and Applications in Light-Emitting Devices. *ACS Appl. Mater. Interfaces* **2019**, *11*, 1228–1238. [[CrossRef](#)]
17. Kour, R.; Arya, S.; Verma, S.; Singh, A.; Mahajan, P.; Khosla, A. Review—Recent Advances and Challenges in Indium Gallium Nitride (InGaIn-xN) Materials for Solid State Lighting. *ECS J. Solid State Sci. Technol.* **2019**, *9*, 015011. [[CrossRef](#)]
18. Pristovsek, M.; Kadir, A.; Meissner, C.; Schwaner, T.; Leyer, M.; Stellmach, J.; Kneissl, M.; Ivaldi, F.; Kret, S. Growth mode transition and relaxation of thin InGaIn layers on GaIn (0001). *J. Cryst. Growth* **2013**, *372*, 65–72. [[CrossRef](#)]
19. Pristovsek, M.; Stellmach, J.; Leyer, M.; Kneissl, M. Growth mode of InGaIn on GaIn (0001) in MOVPE. *Phys. Status Solidi (C)* **2009**, *6*, S565–S569. [[CrossRef](#)]
20. Leyer, M.; Stellmach, J.; Meissner, C.; Pristovsek, M.; Kneissl, M. The critical thickness of InGaIn on (0001)GaIn. *J. Cryst. Growth* **2008**, *310*, 4913–4915. [[CrossRef](#)]
21. Nakatsu, Y.; Nagao, Y.; Hirao, T.; Hara, Y.; Masui, S.; Yanamoto, T.; Nagahama, S.I.; Morkoç, H.; Fujioka, H.; Schwarz, U.T. Blue and green InGaIn semiconductor lasers as light sources for displays. In *Gallium Nitride Materials and Devices XV*; SPIE: Bellingham, WA, USA, 2020.
22. Meissner, C.; Ploch, S.; Pristovsek, M.; Kneissl, M. Volmer-Weber growth mode of InN quantum dots on GaIn by MOVPE. *Phys. Status Solidi (C)* **2009**, *6*, S545–S548. [[CrossRef](#)]
23. Ivaldi, F.; Meissner, C.; Domagala, J.; Kret, S.; Pristovsek, M.; Högele, M.; Kneissl, M. Influence of a GaIn Cap Layer on the Morphology and the Physical Properties of Embedded Self-Organized InN Quantum Dots on GaIn(0001) Grown by Metal–Organic Vapour Phase Epitaxy. *Jpn. J. Appl. Phys.* **2011**, *50*, 031004. [[CrossRef](#)]
24. Grandjean, N.; Massies, J. Real time control of InGaIn-xN molecular beam epitaxy growth. *Appl. Phys. Lett.* **1998**, *72*, 1078–1080. [[CrossRef](#)]
25. Adelman, C.; Simon, J.; Feuillet, G.; Pelekanos, N.T.; Daudin, B.; Fishman, G. Self-assembled InGaIn quantum dots grown by molecular-beam epitaxy. *Appl. Phys. Lett.* **2000**, *76*, 1570–1572. [[CrossRef](#)]
26. Alghoraibi, I.; Rohel, T.; Bertru, N.; Le Corre, A.; Létoublon, A.; Caroff, P.; Dehaese, O.; Loualiche, S. Self-assembled InAs quantum dots grown on InP (3 1 1)B substrates: Role of buffer layer and amount of InAs deposited. *J. Cryst. Growth* **2006**, *293*, 263–268. [[CrossRef](#)]

27. Jiang, L.; Liu, J.; Zhang, L.; Qiu, B.; Tian, A.; Hu, L.; Li, D.; Huang, S.; Zhou, W.; Ikeda, M.; et al. Suppression of substrate mode in GaN-based green laser diodes. *Opt. Express* **2020**, *28*, 15497–15504. [[CrossRef](#)] [[PubMed](#)]
28. Oliver, R.A.; Kappers, M.J.; Humphreys, C.J.; Briggs, G.A.D. The influence of ammonia on the growth mode in InGaN/GaN heteroepitaxy. *J. Cryst. Growth* **2004**, *272*, 393–399. [[CrossRef](#)]

Disclaimer/Publisher’s Note: The statements, opinions and data contained in all publications are solely those of the individual author(s) and contributor(s) and not of MDPI and/or the editor(s). MDPI and/or the editor(s) disclaim responsibility for any injury to people or property resulting from any ideas, methods, instructions or products referred to in the content.